CEN-161 (B)-NP

IMPROVEMENTS TO FUEL EVALUATION MODEL

JULY, 1981

POWER SYSTEMS
COMBUSTION ENGINEERING, INC.

CEN-161(B)-NP

IMPROVEMENTS TO FUEL EVALUATION MODEL

REACTOR DESIGN
FUELS DEVELOPMENT

JULY, 1981

Combustion Engineering, Inc.

ABSTRACT

A new version of the FATES fuel performance code has been developed which gives improved predictions of fuel rod temperature distributions and internal gas pressures as a function of mechanical design and operating history. The improvements to FATES are of particular significance at high fuel burnups.

This report describes the new models which have been incorporated in the improved version, denoted as FATES3, the most significant of which is a new fission gas release model. A data base is provided which demonstrates the predictive capability of the FATES3 code.

TABLE OF CONTENTS

TABLE OF CONTENTS

LIST OF TABLES

LIST OF FIGURES

LIST OF FIGURES

1.0 INTRODUCTION

1.1 PURPOSE

The purpose of this report is to describe the improvements made to the Combustion Engineering (C-E) fuel performance analysis code, FATES, which is a component of the C-E Fuel Evaluation Model described in Reference 1-1. The improved code version is referred to as FATES3.

FATES3 is used to predict fuel rod temperature distributions and internal gas pressures as a function of mechanical design and operating history. Results from FATES3 are used in fuel rod design (e.g., for setting initial fill gas pressure) and safety analyses.

This report will:

a. Describe the additions and modifications to the FATES fuel performance code, which have resulted in the new code version referred to as FATES3.

b. Describe the experimental data base used to develop the new models incorporated in FATES3.

c. Provide comparisons of FATES3 predictions with experimental data from commercial and test reactors.

1.2 SCOPE AND DESCRIPTION

C-E compiles and reviews fuel behavioral data from the open literature and its own programs on a continuing basis in order to better understand fuel behavior and to develop new models for incorporation in its fuel performance codes. Data developed since 1974, the date of inception of the FATES model, extend to higher burnups and are applicable to a wider variety of operating conditions. The improvements made to FATES which more accurately predict fuel behavior, especially at high burnup, are in the following areas:

- fission gas release
- fuel pellet swelling
- pellet-clad interface treatment
- fuel relocation

In addition, the capability of modeling annular fuel pellets has been included in FATES3. This capability is particularly useful for the prediction of fuel temperatures in experimental rods where centerline thermocouples have been incorporated to produce temperature measurements, and in the evaluation of the performance of advanced fuel designs containing annular fuel pellets.

The plenum gas temperature and clad axial irradiation growth were input to the previous FATES code version. These calculations are performed internally in FATES3. Axial growth is calculated with a previously approved model.

The most significant improvement to FATES is in the area of fission gas release modeling. The fission gas release rate depends on the amount of retained fission gas, burnup, temperature, and fuel grain size. Fission gas release concomitant with fuel grain growth is also taken into account.

Fuel pellet swelling consists of solid and gaseous components and commences after maximum fuel densification is reached at 4000 MWD/MTU. The gaseous component decreases fuel density and decreases fuel thermal conductivity. Fuel density was held constant after 4000 MWD/MTU in the previous version of FATES. A new value for the overall fuel volumetric swelling rate also has been incorporated.

The previous FATES model used a preassigned limit on gap conductance in lieu of an explicit treatment of the pellet-clad interface. A model has been incorporated in FATES3 which explicitly treats pellet-clad mechanical interaction. The gap conductance is no longer limited to the values given in Reference 1-1.

Fuel pellet relocation is a term used to describe the outward displacement of pellets into the gap region between fuel and clad resulting from fuel cracking. The FATES3 pellet relocation model is the model originally proposed in Reference 1-1.

1.3 REFERENCES FOR SECTION 1.0

1-1 Combustion Engineering, Inc., "C-E Fuel Evaluation Model Topical Report", CENPD-139, July, 1974. (Proprietary)

2.0 FISSION GAS RELEASE

2.1 INTRODUCTION

The prediction of fission gas release is important in the evaluation of fuel performance because gas conductivities, fuel temperatures and fuel rod internal pressures are dependent on the amount of fission gas released from the fuel. An empirical model to calculate fission gas release was developed by C-E for use in FATES and was described in CENPD-139 (Ref. 2-1). The model was calibrated against the data from UO_2 fuel available at that time which were limited to burnups below 10,000 MWD/MTU. Although from theoretical considerations, fission gas release is known to be dependent on temperature, burnup and fuel microstructure, the lack of a sufficiently well-characterized data base precluded a separation of the effects of these variables on gas release. As a result, temperature was used as the only explicit variable in most LWR models for fission gas release (Ref. 2-2). In the CENPD-139 model, a burnup dependence was indirectly accounted for, in the temperature region below columnar grain growth, by a term which varied with the square root of irradiation time.

Recently, with the availability of some gas release data at higher burnups, the burnup effects on gas release have received increased attention (Ref. 2-3). A review of some of these data led the NRC to conclude that the burnup sensitivity of gas release is stronger than recognized earlier. C-E initiated an analytical and experimental investigation of fission gas release. Emphasis was placed on well characterized fuel rods representing modern PWR's and irradiated over a wide range of monitored parameters.

The new model presented herein accounts for the effects of temperature, burnup, and grain size. The model is described and the comparisons with experimental data are also presented.

2.2 SUMMARY

In the C-E fission gas release model, gas release is calculated by following the local inventory of retained fission gas in the fuel. At each axial region of the fuel column, the fuel is divided into ten rings of equal thickness and the local inventory of fission gas is followed in each of these rings. Local fuel temperature, burnup, grain size and irradiation history are

variables affecting the inventory of retained fission gas in the following manner:

[ ] (2-1)

(2-2)

(2-3)

The percent of generated fission gas that is released, F, is calculated from:

[ ] (2-4)

The functional relationships assumed in Equations 2-1 and 2-2 are based on an inspection of the shapes of the experimentally determined curves of the retained inventory of fission gas in small UO_2 fuel samples at high burnups (Refs. 2-4 and 2-5). The specific values of the constants in the expression for K, given by Equation 2-2, have been arrived at by correlating the gas release predictions of the overall gas release model, when employed in the FATES3 code, to the experimental

data obtained from the steady state irradiation of commercial fuel rods in Calvert Cliffs-1 (Refs. 2-6 and 2-7) and from ramp tests performed at Studsvik as part of the OVER-RAMP program which included C-E segmented commercial fuel rods irradiated in Obrigheim (Ref. 2-8). The maximum inventory obtained by applying Equation 2-3 is equivalent to the release predicted by the low-temperature gas release model developed by the ANS 5.4 Committee (Ref. 2-9).

Fission gas release that is accompanied by grain growth (via grain boundary sweeping) is accounted for in the model by an additional term which depletes the fission gas previously retained in the volume of fuel which is swept by moving grain boundaries. The local inventory of fission gas that remains in each ring of fuel after a local grain growth from G_i to G_f is given by:

[ ] (2-5)

The kinetics of grain growth are followed in each fuel ring [ ]

[ ] (2-6)

[

]

[

] (2-7)

2.3 DISCUSSION

The basic approach that has been adopted in calculating fission gas release in this model is to follow the retained inventory of fission gas in each of ten radial rings of the fuel in up to 20 axial nodes. The release is then calculated by subtracting the amount of gas retained from the total amount of gas generated. This approach was based on a review of data on retained fission gas in high burnup UO_2 fuels published by Zimmermann of Karlsruhe (Refs. 2-4 and 2-5). These data were generated by utilizing specially designed test rigs for irradiating small and thin discs of UO_2 at nearly isothermal conditions. Fuel temperatures were monitored with thermocouples, and burnups of up to 89 MWD/KgU were achieved by utilizing specimens of 15-20% enrichment. Fuel temperatures ranged from 1100 to 1900°K. These results show that at any temperature, the fission gas retained in the UO_2 fuel increases with burnup and tends to reach a saturation level. The burnup at which the saturation inventory is reached varies with temperature, and the saturated inventory goes down exponentially with increasing temperature. These experimentally observed trends were used as inputs in developing the functional instantaneous dependency of the retained inventory, and the released inventory, of fission gas on fuel temperature and burnup. Figure 2-1 illustrates this relationship for a fuel with an initial grain size of 5 μm based on Equations 2-1 through 2-4.

In addition to temperature and burnup, the dynamic grain size is also used as a variable affecting fission gas retained in the fuel. From theoretical grounds, a grain size effect is believed to originate primarily from the following two factors: 1) variation in the diffusion distance of fission gas to the grain boundaries as a function of grain size and 2) variation in the rate of grain growth with grain size. Experimental support for both of these effects up to 4 MWD/KgU is available from the work of Turnbull (Ref. 2-11). A continued influence of grain size on fission gas release at higher burnups has been documented in a number of C-E publications (Refs. 2-12 and 2-13).

Both aspects of the grain size effect discussed above are treated in the model. [

] This effect is illustrated in Figure 2-2 for fuels of various grain sizes at a burnup of 24 MWD/KgU, based on Equations 2-1 through 2-4. The grain growth effect is modeled by incorporating the additional inventory reduction term of Equation 2-5, which accounts for fission gas release caused by grain boundary sweeping.

[

] Figure 2-3 shows the number of hours necessary to achieve an equilibrium grain size for various starting grain sizes and local fuel temperature when these equations are employed. Figures 2-4 through 2-6 show the additional gas release that occurs through the grain growth mechanism depending on time at temperature and the initial grain size (the zero-hour curves represent the instantaneous release contribution previously illustrated alone in Figure 2-2). Figures 2-7 and 2-8 show the instantaneous and grain growth portions of gas release when integrated across a fuel pellet cross section at 10 and 25 MWD/KgU for instantaneous transients from a power level of 10 kw/ft.

2.4 APPLICATION TO A VARIABLE FUEL TEMPERATURE HISTORY

[

]

[

]

[

]

[

]

[

] (2-8)

[

]

[

]

[

]

2.5 CORRELATION DATA BASE AND RESULTS

The dependencies of the fission gas release model on burnup, temperature and grain size were established by correlating the model predictions with measured gas release data from two different sources (a steady state irradiation source and a ramp test data source). Both sources include prepressurized PWR fuel rods that were fabricated by C-E. The final correlation which resulted in the model presented herein was done through the explicit use of this model in the FATES3 code and consisted of establishing the final form of the burnup dependence in Equation 2-1 and the values of the constants in Equation 2-2. The results of the correlation exercise are discussed in this section. Additional data comparisons have been made to verify the model against an independent data base in Section 9.0.

The correlation data base included:

--[ ]measured gas release values from full-length prepressurized C-E fuel rods irradiated at Calvert Cliffs-I through 1 to 3 cycles

--[ ]measured gas release values from C-E and KWU fuel rod segments irradiated at Obrigheim through 1 to 3 cycles, and subsequently ramp tested without failure at the R-2 reactor as part of the Studsvik OVER-RAMP Program

--[ ]measured gas release values from fuel rods irradiated at BR-3 during Cycle 4A and subsequently ramp tested without failure at the R-2 reactor, also as part of the OVER-RAMP Program.

The important design and operating variables as well as comparisons of measured and FATES3 predicted gas release values are summarized for these data sources in Tables 2-1 through 2-4. The rods included represent a range in peak burnup [ ]a range in peak LHGR[ ]and a range

in initial grain size[ ] A summary of the comparisons of measured and predicted fission gas release is given in Figure 2-10 for all[ ]rods in the correlation data base. This figure demonstrates the excellent prediction capability of the FATES3 code with the use of C-E's new gas release model.

It is noted that fission gas release from the Calvert Cliffs - I rods having an old-type densifying fuel is more conservatively predicted as a group.[

]

2.6 REFERENCES FOR SECTION 2.0

2-1 Combustion Engineering, Inc., "C-E Fuel Evaluation Model Topical Report", CENPD-139, July, 1974. (Proprietary)

2-2 Core Performance Branch, USNRC, "The Role of Fission Gas Release in Reactor Licensing", NUREG-75/077, November 1975.

2-3 R. O. Meyer, C. E. Beyer and J. C. Voglewede, "Fission Gas Release from Fuel at High Burnup", Office of Nuclear Reactor Regulation, USNRC, NUREG-0418, March 1978.

2-4 H. Zimmermann, "Investigation of Swelling and Fission Gas Retention on Oxide Nuclear Fuel Under Neutron Irradiation", Kernforschungszentrum, Karlsruhe, KFK-2467, June 1977.

2-5 H. Zimmermann, "Investigation of Swelling and Fission Gas Behavior in Uranium Dioxide", J. Nucl. Mat., Vol. 75 (1978) pp. 154-161.

2-6 S. R. Pati, "Gas Release and Microstructural Evaluation of One-and Two-Cycle Fuel Rods from Calvert Cliffs-I", Combustion Engineering, Inc., NPSD-75, March 1979.

2-7 S. R. Pati, "Gas Release and Microstructural Evaluation of Three-Cycle Fuel Rods from Calvert Cliffs - I", Combustion Engineering, Inc., C-E NPSD-119, December 1980.

2-8 T. Hollowell et. al., "The International Over-Ramp Project at Studsvik, Proposed Paper for ANS Topical Meeting on LWR Extended Burnup Fuel Performance and Utilization,"April 4-8, 1982, Williamsburg, Virginia.

2-9 ANSI/ANS-5.4, "Proposed American National Standard Method for Calculating the Release of Fission Products from Oxide Fuels", ANS 5.4, Draft, November, 1979.

2-10 J. B. Ainscough, B. W. Oldfield and J. O. Ware, "Isothermal Grain Growth Kinetics in Sintered UO_2 Pellets", J. Nucl. Mat. Vol. 49 (1973/74) pp. 117-128.

2-11 J. A. Turnbull, "The Effect of Grain Size on the Swelling and Gas Release Properties of UO_2 During Irradiation", J. Nucl. Mat. Vol. 50 (1974) pp. 62-68.

2-12 S. R. Pati, "Structure Sensitivity of Fission Gas Release in LWR Fuels", American Ceramic Society Bulletin, Vol. 56, No. 8 (1977) p. 735.

2-13 S. R. Pati, "Gas Release and Fuel Microstructure", American Ceramic Society Bulletin, Vol. 57, No. 3 (1978), p. 357.

2-14 F. Sontheimer, P. Dewes, and H. Knaab, "Correlating Fission Gas Release Due to Power Ramping with Observed Microstructural Changes in the Fuel by Use of a Simple Diffusion Model", Paper Presented at the Enlarged Halden Programme Group Meeting on Water Reactor Fuel Performance", June 14-19, 1981.(Proprietary)

Table 2-1

The Correlation Data Base-
FATES3 Predictions of Gas Release From Calvert Cliffs-I Rods

Rod Number	Fuel Stability to In-Reactor Densification	Initial Grain Size, μm	Peak LHGR kw/ft(BOL)	Rod Averaged Burnup Mwd/kgU	% Gas Release	
					Measured	Predicted
01	Densifying	2.5	9.1	18.7	0.27	8.25
46	Nondensifying	15	11.1	21.6	0.71	0.84
50	Nondensifying	4	9.1	18.7	0.33	1.41
05	Densifying	2.5	9.1	25.8	0.34	6.71
47	Nondensifying	15	11.1	29.1	0.64	0.72
51	Nondensifying	4	9.1	25.8	0.35	1.15
11	Densifying	2.5	9.1	33.0	0.36	5.53
12	Densifying	2.5	9.1	33.0	0.35	5.46
39	Nondensifying	15	11.1	37.0	0.71	0.61
42	Nondensifying	15	11.1	37.0	0.72	0.69
53	Nondensifying	4	9.1	33.0	0.33	1.00
60	Nondensifying	7	9.1	33.0	0.59	0.84

Table 2-2

The Correlation Data Base

FATES3 Predictions of Gas Release From Over-Ramp Program Rods

Rod Number	Initial Grain Size, μm	Ramp Peak LHGR, kw/ft[a,b]	Rod Averaged Burnup, Mwd/kgU	% Gas Release	
				Measured	Predicted
[					]

a [

]

b [

]

Table 2-3

Summary of Design Parameters
For Rods in the Correlation Data Base

Parameter	Over-Ramp	Calvert Cliffs 1
Clad OD, IN	[	.440
Clad ID, IN		.388
Initial Pellet-Clad Diametral Gap, Mils		8.5
Initial Grain Size, μm		2.5 - 15
Fuel Column Length, IN		136.7
Initial Fuel Density , % TD		93 - 95
Fill Gas Pressure at 70°F, psia*		315 , 465
Enrichment, % U235	]	2.5 , 2.8

[ ]

Table 2-4

Summary of Thermal-Hydraulic Parameters
For Rods in the Correlation Data Base

Parameter	Over-Ramp*	Calvert Cliffs 1
Coolant Pressure, psia	[ ]	2250
Coolant Inlet Temperature, ^{o}F	[ ]	548

*The coolant pressure and inlet temperature during power ramping are [ ] psia and [ ] respectively.

Figure 2-1 Instantaneous Portion of the Total Fission Gas Release

Figure 2-2 Grain Size Dependence of the Instantaneous Fission Gas Release

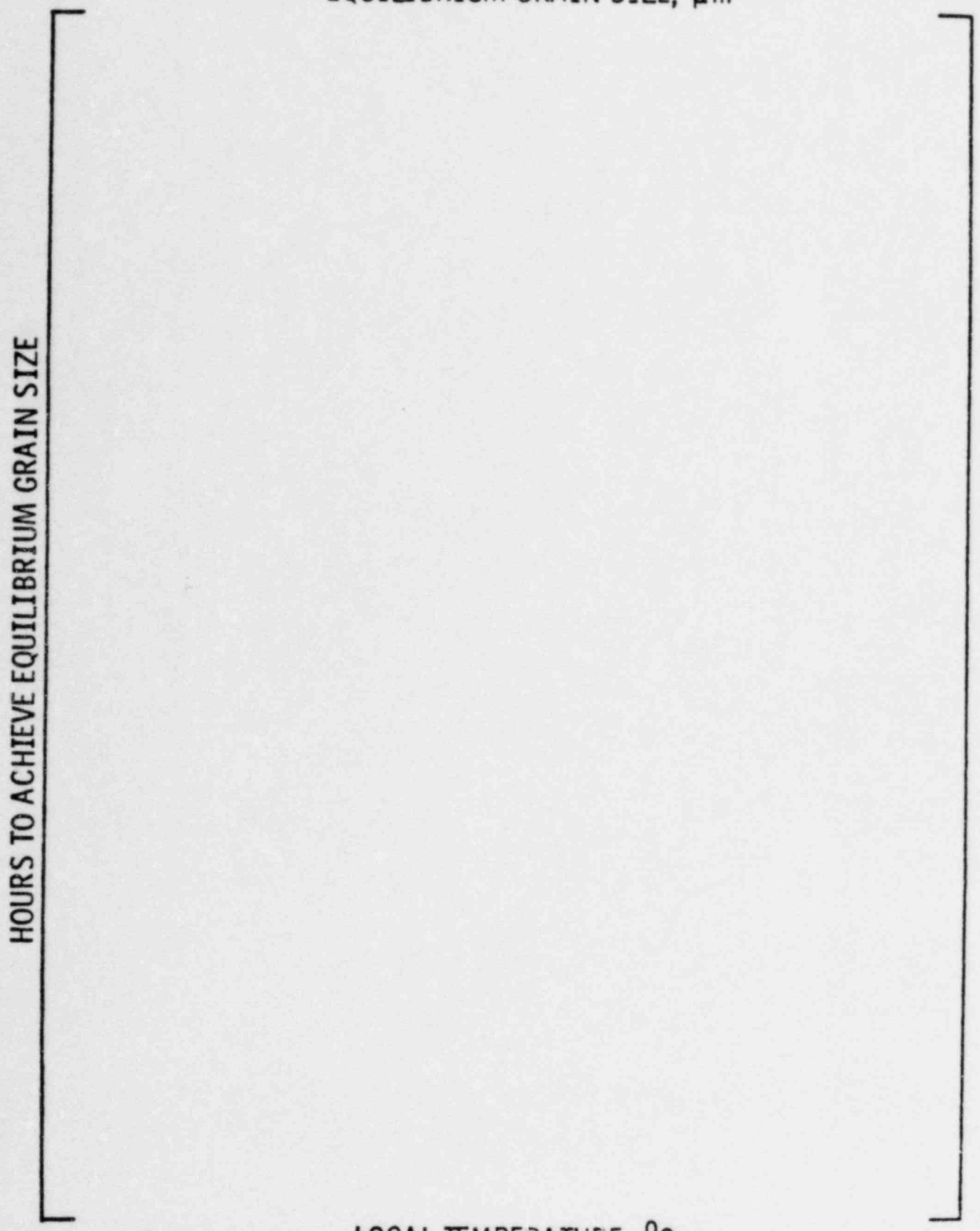

Figure 2-3 Time to Achieve an Equilibrium Grain Size as a Function of Initial Grain Size and Local Fuel Temperature

LOCAL FISSION GAS RELEASE, %

LOCAL FUEL TEMPERATURE, °C

Figure 2-4 Instantaneous and Grain Growth Related Portions of the Total Fission Gas Release as Functions of Local Fuel Temperature and Time at Temperature for a 5 μm Initial Grain Size

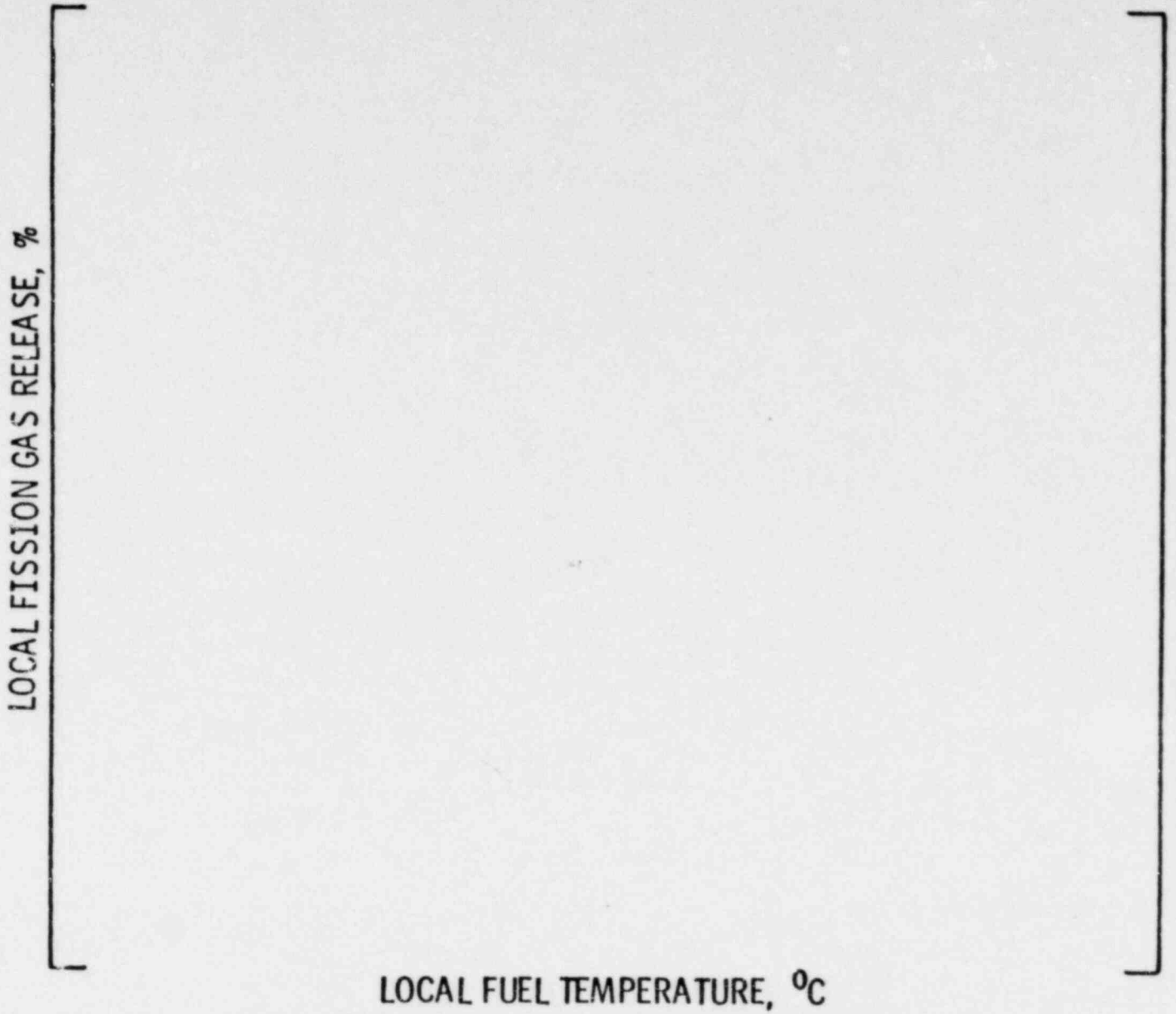

Figure 2-5 Instantaneous and Grain Growth Related Portions of the Total Fission Gas Release as Functions of Local Fuel Temperature and Time at Temperature for a 10 μm Initial Grain Size

LOCAL FISSION GAS RELEASE, %

LOCAL FUEL TEMPERATURE, °C

Figure 2-6 Instantaneous and Grain Growth Related Portions of the Total Fission Gas Release as Functions of Local Fuel Temperature and Time at Temperature for a 20 μm Initial Grain Size

Figure 2-7

POWER AND TIME DEPENDENCE OF FISSION GAS RELEASE
AT 10 MWD/KGU

Figure 2-8

POWER AND TIME DEPENDENCE OF FISSION GAS RELEASE AT 25 MWD/KGU

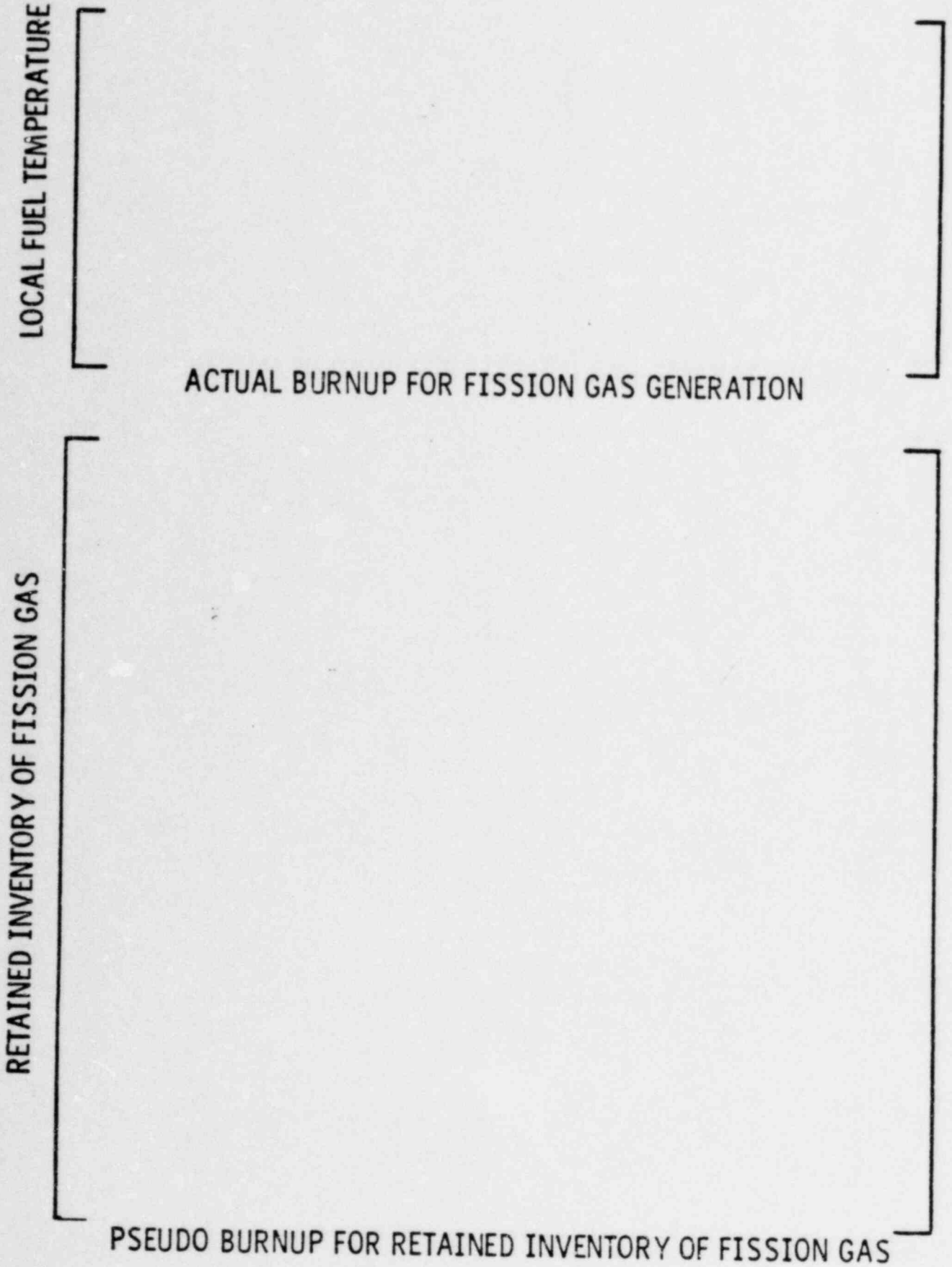

Figure 2-9 Example Application of the Gas Release Model to a Variable Temperature History

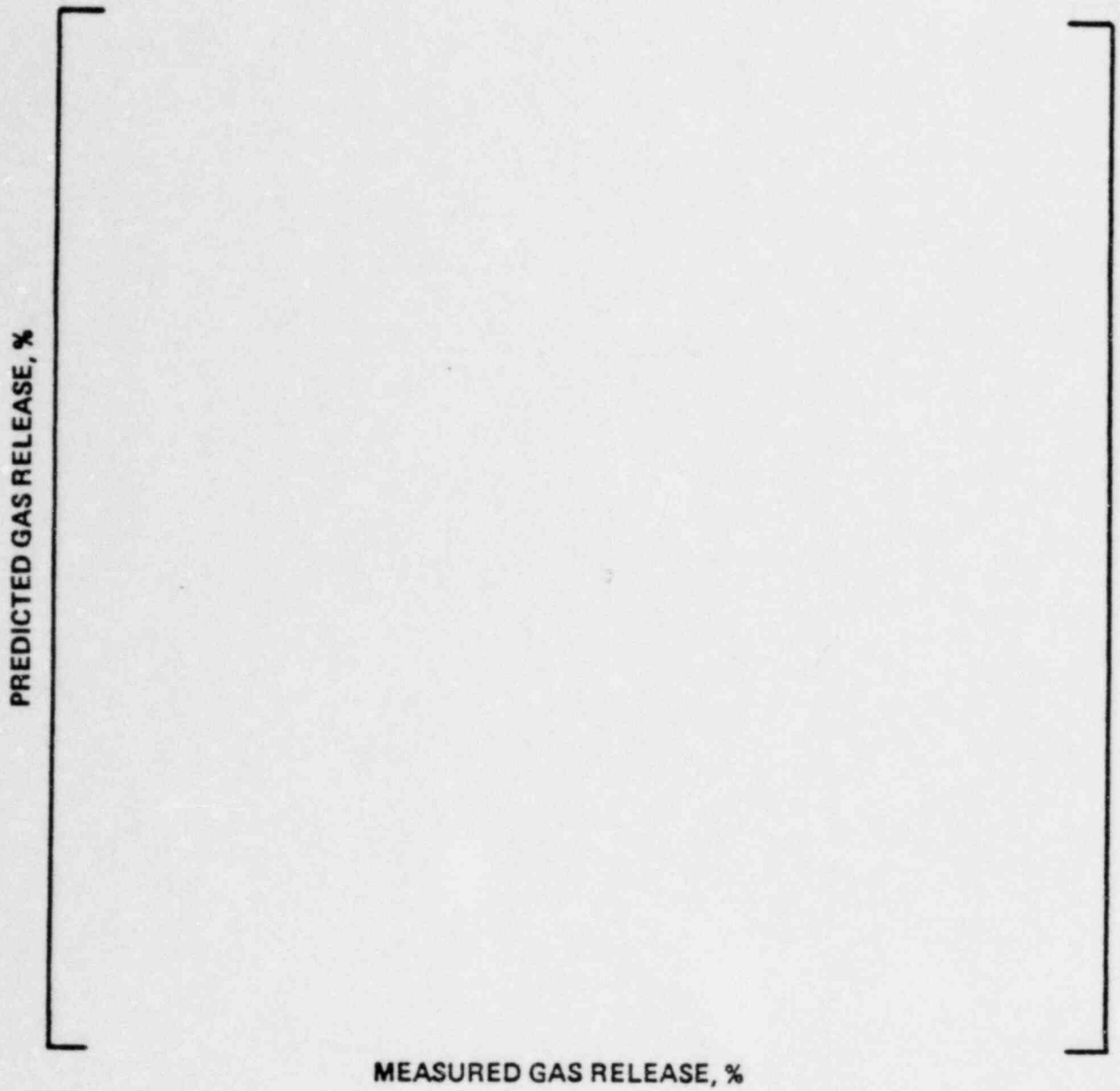

Figure 2-10 A Comparison of FATES3 Predictions with Measured Fission Gas Release from Calvert Cliffs I Rods and Studsvik OVER-RAMP Rods (The Model Correlation Data Base)

3.0 FUEL PELLET SWELLING

3.1 INTRODUCTION

The fuel swelling model in FATES has been revised by taking into consideration some of the recent data in the open literature as well as the data on post-irradiation density changes of C-E fuels irradiated in Calvert Cliffs-1 through three cycles. These data indicate that in the range of commercial operation, the unrestrained swelling rate of LWR fuels is lower than the rate used in Reference 3-1. The technical basis for the modification of the swelling rate is discussed below.

3.2 DISCUSSION

The previous model for calculating diametral swelling of fuel pellets in FATES (Ref. 3-1) assumed isotropic swelling in the burnup range from 4,000 MWD/MTU until hard contact occurs between fuel and cladding. The diametral swelling rate was set equal to one-third the pellet average volumetric rate of 0.6% $\Delta V/V$ per 4,000 MWD/MTU burnup. The basis for this volumetric swelling rate was the data on plate fuel elements obtained by Bettis in the early 1960s (Ref. 3-2). These data were reanalyzed by Rowland et al (Ref. 3-3), and swelling rates of 0.3 to 0.5% $\Delta V/V$ per 4,000 MWD/MTU were obtained by a least-squares fit of the data. Additional data and analyses were also presented by these authors which suggested that the typical swelling rate for LWR fuels would be significantly lower than that originally published by Bettis. For example, precise measurements of UO_2 fuel rods irradiated in GETR up to 91,000 MWD/MTU yielded a swelling rate of 0.4% $\Delta V/V$ per 4,000 MWD/MTU. A number of other investigators also reported swelling rates in UO_2 which are lower than the value used before. For example, Brucklacher and Dienst (Ref. 3-4) derived a rate of 0.32%$\Delta V/V$ per 4,000 MWD/MTU from in-pile creep measurements. Collins and Hargreaves (Ref. 3-5) reported that measurements on high-burnup fuel yield a swelling rate of 0.2% $\Delta V/V$ per 4,000 MWD/MTU, whereas interpretation of length changes of fuel pins irradiated in Windscale AGR yielded a rate of 0.4% $\Delta V/V$ per 4,000 MWD/MTU.

More recently, the swelling behavior of a number of PWR fuels have been characterized by analyzing the changes in density of fuel pellets as a

function of burnup. Data presented by Assmann and Manzel of KWU (Ref. 3-6) for standard fuel of 95% TD showed a pore-free matrix swelling rate of 0.4% per 4,000 MWD/MTU in the burnup range of 12,000 to 45,000 MWD/MTU.

High burnup swelling characteristics of three fuel types (one densifying and two nondensifying fuels) were recently characterized by C-E (Ref. 3-7) as part of an EPRI program. The swelling rates were deduced by analyzing the rates of density decreases of these fuels as a function of burnup in the range of 20,000 to 41,000 MWD/MTU. Specimens for density measurements were taken from fuel rods with two and three cycles in Calvert Cliffs-1. To minimize the perturbation from in-reactor densification, only the data above 20,000 MWD/MTU burnup were used. Each of the three fuel types showed lower bulk swelling rates than the pore-free matrix swelling rate of 0.4% $\Delta V/V$ per 4,000 MWD/MTU. The observed variation in the bulk swelling rate was related to the variations in the fuel microstructure. For example, the 93% TD nondensifying fuel showed the lowest bulk rate of 0.24% per 4,000 MWD/MTU compared to the highest observed rate of 0.37% per 4,000 MWD/MTU in the 95% TD nondensifying fuel. It is believed that the lower swelling rate of the lower density fuel resulted from greater swelling accommodation in this fuel type. Higher swelling accommodation in this fuel was facilitated by the presence of a large fraction of initial porosity as open pores distributed in the inter-agglomerate region of the pellet microstructure. These results indicate that although the bulk swelling rate deduced from post-irradiation immersion densities may vary appreciably due to different degrees of swelling accommodations, the rate of 0.4% $\Delta V/V$ per 4,000 MWD/MTU provides a good estimate of the unrestrained swelling rate of UO_2 fuel at high burnups. This unrestrained rate is equivalent to the swelling rate of a pore-free matrix published by Assmann and Manzel (Ref. 3-6).

Further justification for the swelling rate selected is available from the good agreement that is observed between the internal fuel rod void volume calculated by using this swelling rate and the void volume measured in twelve Calvert Cliffs-1 fuel rods. The internal void volumes of these rods were measured in a hot cell at the end of each of the first three cycles of irradiation (Refs. 3-8 and 3-9). Fuels from the two- and three-cycle rods from this group were subsequently used for post-irradiation density measurements discussed above. These fuel rods were well characterized in terms of the as-fabricated dimensions, fuel pellet attributes, and detailed irradiation histories. The beginning-of-life

(BOL) void volumes were estimated from puncturing archive rods, from the initial as-fabricated dimensions and from the open porosity measured in archive fuel pellets (Refs. 3-8 and 3-9). The dimensional changes of the fuel rods, during irradiation were measured during poolside inspections (Refs. 3-10 and 3-11). The void volume changes due to fuel densification were estimated by an upward adjustment of the resintering test data so that a higher estimate of the fuel swelling is obtained. The void volumes at the end of each cycle were calculated by FATES3 following the detailed power histories. As shown in Section 9.1 good agreement exists between the predicted and measured void volumes.

The above considerations provide a basis for the use of an unrestrained swelling rate of 0.4% $\Delta V/V$ per 4,000 MWD/MTU. No change in the swelling model (Ref. 3-1) has been made in the range of zero to 4,000 MWD/MTU (i.e., no swelling is assumed below 4,000 MWD/MTU) and after fuel-cladding contact is predicted to occur by FATES3. Since the two- and three-cycle Calvert Cliffs-1 fuel rods operated well beyond the onset of fuel-cladding contact, and the predicted void volumes agree well with the measured void volumes, the integrated swelling model (including accommodation of swelling volume in closed and open pores, into dishes, and the fuel-clad gap) is, therefore, inferred to be valid to a significant range of burnup (38 MWD/KgU rod average).

During periods of pellet-clad contact, the difference between restrained and unrestrained swelling fills the fuel column internal voids in proportion to BOL amounts of internal volume.

The total swelling rate of 0.4% $\Delta V/V$ per 4,000 MWD/MTU results from the combination of swelling due to solid and gaseous fission products. Theoretical estimates of solid fission product swelling in UO_2 vary from 0.13 to 0.35% $\Delta V/V$ per 4,000 MWD/MTU (Refs. 3-12, 3-13, and 3-14). The minimum rate of these estimates is generally obtained by assuming a complete utilization of vacancies created by fissioning of uranium atoms and the maximum rate by assuming no utilization. The average of the above estimate, 0.24% $\Delta V/V$ per 4,000 MWD/MTU, is taken as the volumetric swelling rate due to solid fission products. The remaining swelling rate of 0.16% $\Delta V/V$ per 4,000 MWD/MTU is assumed to be due to gaseous fission products and is used to reduce fuel density and, therefore, fuel conductivity, beyond 4,000 MWD/MTU. Gaseous fission product swelling was not treated in the previous FATES code version.

Figure 3-1 shows fuel density as a function of burnup for the combined fuel densification (Ref. 3-1) and swelling models. The assumed densification change is 1.6% of theoretical density (TD) for this example.

3.3 REFERENCES FOR SECTION 3.0

3-1 Combustion Engineering, Inc., "C-E Fuel Evaluation Model Topical Report", CENPD-139, July, 1974. (Proprietary)

3-2 R. C. Daniel, M. L. Bleiberg, H. B. Meieran and W. Yeniscavitch, Bettis Atomic Laboratories, WAPD-263, 1962.

3-3 T. C. Rowland, M. O. Marlowe and R. B. Elkins, "Fission Product Swelling in BWR Fuels", Tran. Am. Nucl. Society, Vol. 18 (1974) 124.

3-4 D. Brucklacher and D. W. Dienst, J. Nucl. Mat. Vol. 42 (1972) 285

3-5 D. A. Collins and R. Hargreaves, "Performance Limiting Phenomena in Irradiated UO_2", BNES Conf. London (1973) 50.1

3-6 H. Assmann and R. Manzel, Kraftwerk Union AG, "The Matrix Swelling Rate of UO_2", J. Nucl. Mat. Vol. 68 (1977) 360-364.

3-7 N. Fuhrman and P. A. Van Saun, Combustion Engineering, Inc., "Densification and Swelling Behavior of Two- and Three-Cycle UO_2 Fuels from Calvert Cliffs-1", CE NPSD-135, March 1961.

3-8 S. R. Pati, Combustion Engineering, Inc., "Gas Release and Microstructural Evaluation of One- and Two-Cycle Fuel Rods from Calvert Cliffs-1", NPSD-75, March, 1979.

3-9 S. R. Pati, Combustion Engineering, Inc., "Gas Release and Microstructural Evaluation of Three-Cycle Fuel Rods from Calvert Cliffs-1", C-E NPSD-119, December, 1980.

3-10 D. E. Bessette, et al, Combustion Engineering, Inc., "Examination of Calvert Cliffs-1 Test Fuel Assemblies at End of Cycles 1 and 2," NPSD-72, September, 1978.

3-11 E. J. Ruzauskas, J. G. Schneider and P. A. Van Saun, Combustion Engineering, Inc., "Examination of Calvert Cliffs-1 Test Assemblies after Cycle 3", NPSD-87, September, 1979.

3-12 Ansilin, "The Role of Fission Products in the Swelling of Irradiated UO_2 and U, Pu) O_2 Fuel", GEAP-5583, 1969.

3-13 Findlay, J. R., "Calculations of Fission Products Swelling in Oxide and Carbide Fuels", AERE M-1943 (1967).

3-14 Ewart, F. T., Private Communication as Referred to in Reference 3-5.

Figure 3-1

Fuel Density versus Burnup for an Assumed Fuel Densification of 1.6% TD

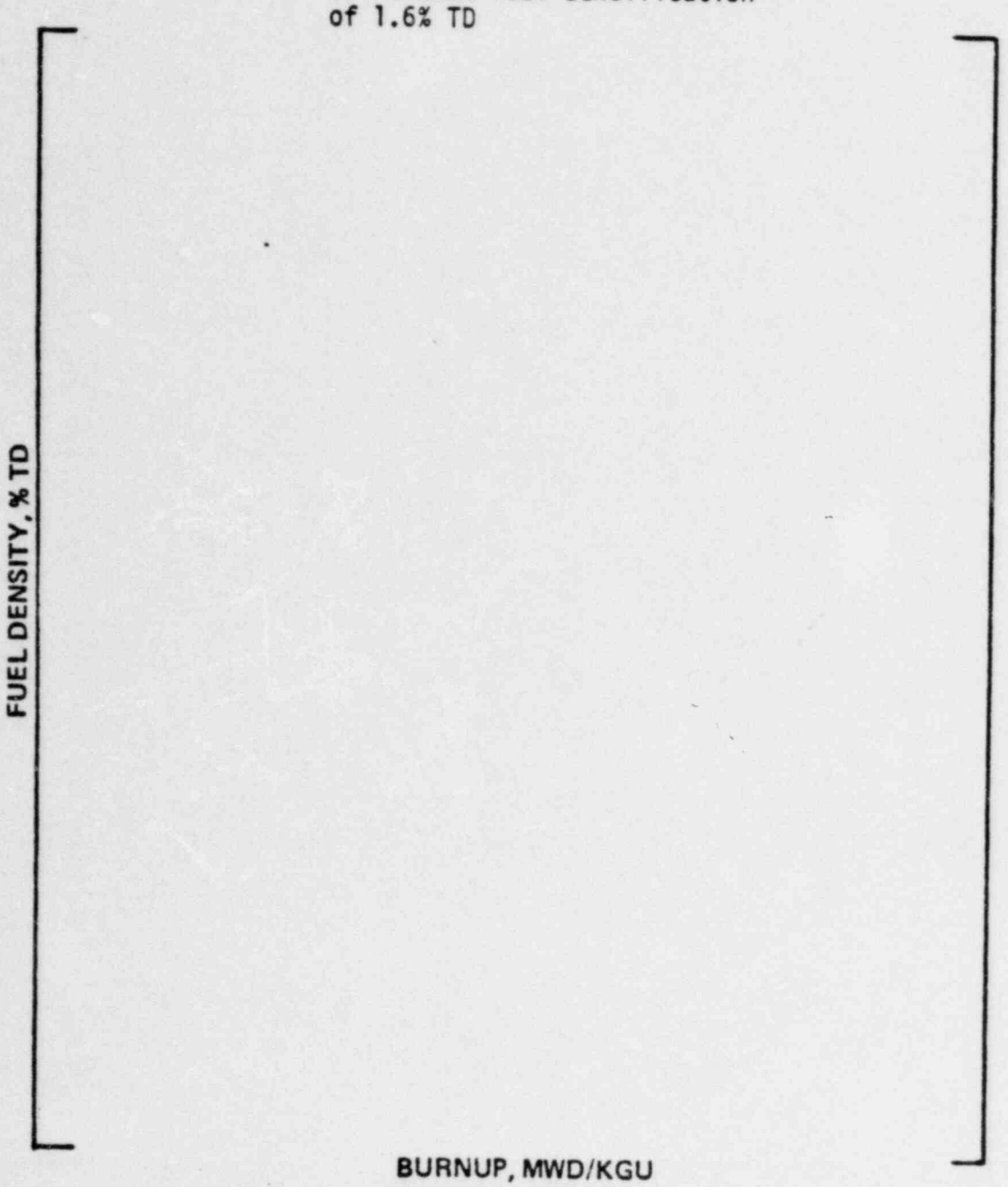

4.0 FUEL-CLAD INTERFACE

4.1 INTRODUCTION

The previous FATES model used preassigned maximum values for gap conductance and pellet-clad mechanical interfacial pressure in lieu of an explicit treatment of the movement of the pellet-clad interface after pellet-clad contact. A pellet-clad mechanical interaction model, which explicitly treats the interface, has been included in FATES3. This model is described in the following sections.

4.2 PELLET-CLAD CONTACT LOADING

After the pellet and clad make contact, a mechanical interfacial pressure exists which is calculated from the elastic strain necessary to force the clad to conform to the fuel pellet. The interfacial pressure is used in the previous FATES model in the calculation of the contact conductance component of the gap conductance. In FATES3, the interfacial pressure is also used in calculating the hoop stress for the clad creep calculation. The resulting expression for hoop stress is a modified form of Equation 30 in Reference 4-1:

$$\sigma_\theta = [P_g - P_w + P_m]\,[R_1 + R_2]/[2(R_1 - R_2)] \qquad (4\text{-}1)$$

where:

σ_θ = clad hoop stress, psi

P_g = fuel rod internal gas pressure, psi

P_w = reactor coolant pressure, psi

P_m = mechanical interfacial pressure, psi

R_1 = input clad outside radius, in

R_2 = input clad inside radius, in

The mechanical interfacial pressure relaxes through clad creep. All components are calculated such that pellet and clad are in equilibrium.

4.3 GAP CONDUCTANCE

The interfacial pressure calculated by the previous FATES model did not account for creep and necessitated an upper limit on the value of computed gap conductance.

An upper limit on gap conductance is not used in FATES3 because of the inclusion of an explicit treatment of the pellet-clad interface. The predictions of experimental data in Section 9.0 and fission gas release model calibration in Section 2.0 were performed without a maximum value.

4.4 REFERENCES FOR SECTION 4.0

4-1 Combustion Engineering, Inc., "C-E Fuel Evaluation Model Topical Report", CENPD-139, July, 1974. (Proprietary)

5.0 ANNULAR FUEL PELLETS

5.1 INTRODUCTION

The capability of modeling annular fuel pellets has been included in FATES3. The models used to calculate the fuel pellet temperature distribution, fuel pellet thermal expansion, and rod internal void volume have been modified for annular fuel pellets. These changes are discussed in the following sections.

5.2 TEMPERATURE DISTRIBUTION

The derivation of the equations used to calculate the radial power and temperature distributions for annular fuel pellets is given in this section.

As is the case for solid fuel pellets in Reference 5-1, the radial power distribution in an annular fuel pellet is assumed to be described by:

$$q'''(r/r_o) = q'''_o \left[A+B\left(\frac{r}{r_o}\right)^2 + C\left(\frac{r}{r_o}\right)^4\right] \qquad (5\text{-}1)$$

where:

q''' = local volumetric heat generation rate, BTU/hr-ft^3

q'''_o = volumetric average heat generation rate in the fuel, clad, and moderator, BTU/hr-ft^3

A,B,C = flux depression constants

r/r_o = dimensionless pellet radius

r_o = pellet outer radius, inches

Conservation of energy requires that:

$$\frac{\int_{r_h}^{r_o} \left[A+B\left(\frac{r}{r_o}\right)^2 + C\left(\frac{r}{r_o}\right)^4\right] r\, dr}{\int_{r_h}^{r_o} r\, dr} = 1.0 \qquad (5\text{-}2)$$

where:

r_h = pellet inner radius, inches

Solving Equation 5-2, the normalized flux depression factors must obey the relation:

$$\left\{A\left[1-\left(\frac{r_h}{r_o}\right)^2\right]+\frac{B}{2}\left[1-\left(\frac{r_h}{r_o}\right)^4\right]+\frac{C}{3}\left[1-\left(\frac{r_h}{r_o}\right)^6\right]\right\}\Big/\left[1-\left(\frac{r_h}{r_o}\right)^2\right]=1.0 \qquad (5\text{-}3)$$

The steady state radial temperature distribution through an annular cylindrical pellet with internal heat generation and temperature dependent thermal conductivity is given by the one-dimensional heat conduction equation:

$$\frac{1}{r}\left[\frac{d}{dr}\left(kr\frac{dT}{dr}\right)\right]=-q'''_o F_f\left[A+B\left(\frac{r}{r_o}\right)^2+C\left(\frac{r}{r_o}\right)^4\right] \qquad (5\text{-}4)$$

where:

k = temperature dependent fuel thermal conductivity, BTU/hr-ft-°F (Ref. 5-1)
F_f = fraction of q'''_o generated in the pellet
T = temperature at radius r, °F

Integrating between r and r_h with the pellet inside surface assumed to be an adiabatic boundary gives:

$$kr\frac{dT}{dr}=q'''_o F_f\left[\frac{A}{2}\left(r^2-r_h^2\right)+\frac{B}{4r_o^2}\left(r^4-r_h^4\right)+\frac{C}{6r_o^4}\left(r^6-r_h^6\right)\right] \qquad (5\text{-}5)$$

Integrating between T_o and T and rearranging gives:

$$\int_o^T k_{95}\,dt=\int_o^{T_o} k_{95}\,dT+\frac{q'_o F_f}{4\pi F_p\left[1-\left(\frac{r_h}{r_o}\right)^2\right]}$$

$$\left\{A\left[1-\left(\frac{r}{r_o}\right)^2+2\left(\frac{r_h}{r_o}\right)^2\ln\left(\frac{r}{r_o}\right)\right]\right.$$

$$+B\left[\frac{1}{4}\left[1-\left(\frac{r}{r_o}\right)^4\right]+\left(\frac{r_h}{r_o}\right)^4\ln\left(\frac{r}{r_o}\right)\right] \qquad (5\text{-}6)$$

$$\left.+C\left[\frac{1}{9}\left[1-\left(\frac{r}{r_o}\right)^6\right]+\frac{2}{3}\left(\frac{r_h}{r_o}\right)^6\ln\left(\frac{r}{r_o}\right)\right]\right\}$$

where:

k_{95} = thermal conductivity of 95% dense UO_2, BTU/hr-ft-°F, (Ref. 5-1)

F_p = Maxwell-Euken fuel thermal conductivity porosity correction factor, (Ref. 5-1)

q'_o = linear heat generation rate in the fuel, clad, and moderator, kw/ft

T_o = pellet surface temperature, °F

Equation 5-6 is used in FATES3 to calculate the fuel pellet temperature distributions in annular fuel pellets.

5.3 THERMAL EXPANSION

The derivation of the equations used to calculate thermal expansion in annular fuel pellets is given in this section. The resulting expressions reduce to those in Reference 5-1 for the case of solid fuel pellets.

Thermal expansion of the uncracked portion of the pellet is computed by finding the radially averaged displacement. At each radial ring, the displacement is computed with the coefficient of thermal expansion defined in Reference 5-1. The displacement in the uncracked portion of the pellet is given by:

$$\Delta R_u = \frac{r_c \int_{r_h}^{r_c} \alpha_f \, T r dr}{\int_{r_h}^{r_c} r \, dr} \qquad (5\text{-}7)$$

where:

ΔR_u = change in pellet radius due to thermal expansion in the uncracked portion of the pellet, inches

r_c = pellet crack radius, taken at the 1400°C isotherm, inches (Ref. 5-1)

α_f = thermal expansion coefficient for UO_2 in/in -°F, (Ref. 5-1)

Integrating Equation 5-7 gives:

$$\Delta R_u = \frac{2 r_c}{(r_c^2 - r_h^2)} \int_{r_h}^{r_c} \alpha_f \, Tr \, dr \qquad (5\text{-}8)$$

The integration required by Equation 5-8 is replaced by the numerical summation in Reference 5-1.

Thermal expansion in the cracked portion of the pellet is identical to that in Reference 5-1.

5.4 VOID VOLUME

The fuel rod internal void volume is adjusted for the presence of a central hole. The central hole volume is referenced to the plenum temperature, as are the other components of void volume in Reference 5-1, as follows:

$$V_h = \sum_{i=1}^{N} \pi L_f^i \, (r_h^i)^2 \, (T_{pg} + 460)/(T_c^i + 460) \qquad (5\text{-}9)$$

where:

V_h = total effective volume in the fuel column central hole, in^3

L_f^i = length of fuel column axial segment i, in

N = total number of fuel column axial segments

r_h^i = fuel pellet inner radius in axial segment i, in

T_{pg} = plenum gas temperature, °F

T_c^i = temperature at the fuel pellet inner radius in axial segment i, °F

The central hole and plenum volumes are also corrected for a fuel centerline thermocouple, if one is present.

5.5 REFERENCES FOR SECTION 5.0

5-1 Combustion Engineering, Inc., "C-E Fuel Evaluation Model Topical Report", CENPD-139. July, 1974. (Proprietary)

6.0 FUEL PELLET RELOCATION

6.1 INTRODUCTION

Fuel pellet relocation accounts for the outward displacement of pellets into the gap region between fuel and clad that results from the process of cracking and crack healing. A previously derived relocation model has been included in FATES3 and is described in the following section.

6.2 DISCUSSION

Equation 42 of Reference 6-1 is used to calculate fuel relocation in FATES3. Fuel relocation continued to occur after pellet-clad contact in the previous FATES model. Depending on the specifics of a given duty cycle, all, or part, of the relocation calculated with the referenced equation may be calculated to occur during a given time step in FATES3. All of the relocation is calculated to occur if the hot pellet-clad gap is open. If fuel swelling, thermal expansion, and relocation calculated to occur in previous time steps are sufficient to close the pellet-clad gap, no additional relocation is calculated.

As shown in Section 9.0, use of this relocation model along with the other gap closure models in FATES3 results in good predictions of fuel temperature, fission gas release, and rod internal void volume. Use of this model is, therefore, considered to be appropriate.

6.3 REFERENCES FOR SECTION 6.0

6-1 Combustion Engineering, Inc., "C-E Fuel Evaluation Model Topical Report", CENPD-139, July, 1974. (Proprietary)

7.0 CLAD AXIAL IRRADIATION GROWTH

Irradiation induced axial growth of the clad was numerically input to the previous version of FATES. The model for fuel rods given in Reference 7-1 has been incorporated in FATES3.

7.1 REFERENCES FOR SECTION 7.0

7-1 Combustion Engineering, Inc., "In-Reactor Dimensional Changes in Zircaloy -4 Fuel Assemblies", CENPD-198, December, 1975. (Proprietary)

8.0 PLENUM GAS TEMPERATURE

The fuel rod plenum gas temperature was numerically input to the previous version of FATES. In FATES3, the fuel rod plenum gas temperature is approximated by a weighted average of the fuel pellet volumetric average temperature adjacent to the plenum and the coolant temperature at the channel outlet:

$$T_{pg} = (A_f T_f + A_{pl} T_{co})/(A_f + A_{pl}) \qquad (8\text{-}1)$$

where:

T_{pg} = plenum gas temperature, °F

A_f = cross sectional area of pellet adjacent to end plenum, in^2

T_f = volumetric average temperature of pellet adjacent to end plenum, °F

A_{pl} = cylindrical area of end plenum, in^2

T_{co} = channel coolant outlet tempeerature, °F

9.0 PREDICTIONS OF EXPERIMENTAL DATA

9.1 PURPOSE FOR DATA SELECTIONS

The purpose of this section is to demonstrate the accuracy of the predictive capability of the FATES3 fuel performance code by comparing predictions with experimentally measured data. This data was not used in the development of the FATES3 code. Three experimentally measured parameters, which give an excellent measure of a fuel performance code's predictive capability, were selected for comparison. These are:

- fission gas release
- fuel temperature
- fuel rod internal void volume

Fission gas release is important because of its effect on conductivity of the gas in the fuel-clad gap and because of its partial pressure which increases with burnup. Fuel temperature is obviously important since it represents stored energy and is the ultimate parameter being determined by FATES3.

Internal void volume has been selected for comparison because it, along with fission gas release, is very important in the calculation of rod internal pressure.

In assembling the data base, only rods were selected which were well characterized with respect to mechanical design and irradiation history. Fuel rods typical of C-E fuel rod design were used to the maximum extent possible. Of the total of [ ] rods used for verification, [ ] were prepressurized with helium.

A large number of fuel rods of Kraftwerk Union (KWU) design (which are also similar to C-E fuel design) irradiated in the Obrigheim (KWO) and Stade (KKS) commercial PWR's, both pressurized and unpressurized with helium, were used for fission gas release comparisons. Data for these rods, obtained through a technical information exchange agreement between C-E and KWU, were believed to be not as well defined as the remainder of the data base. They are, however, an excellent source of data for rods irradiated under PWR conditions.

A wide variety of irradiation histories are represented in the data base. Many rods experienced duty cycles typical of those encountered in commercial reactors. Rods which were irradiated in a commercial PWR prior to ramp testing in a test reactor were used to verify fission gas release predictive capability for transient power conditions.

Only rods equipped with fuel centerline thermocouples were selected for fuel temperature comparisons. Although temperatures may be inferred from fuel grain growth or other microstructural temperature markers, they are thought to be unsatisfactory due to the inherent uncertainties associated with microstructural changes. Of the [ ] rods selected for temperature comparisons, [ ] are of C-E design. The remainder are of an older, unpressurized design, but have been historically used for fuel temperature comparisons.

Rods irradiated in the Calvert Cliffs 1 commercial PWR were used for rod internal void volume comparisons. These rods were selected because they are C-E designed and are well characterized with respect to both mechanical design and irradiation history.

The following sections describe the verification data base and the results of the comparisons.

9.2 DATA AND RESULTS

Calculations were made for a total of [ ] fuel rods to verify the predictive capability of FATES3. [ ] rods were modeled with detailed design data and irradiation histories. Published fuel temperatures were modeled for calculating fission gas release for the remaining rods. Table 9-1 gives the number of rods in each data set and their uses. The important design and operating variables are summarized in Tables 9-1 through 9-3. Comparisons of measured and predicted fission gas release, fuel temperature, and void volume data are given in Tables 9-4 through 9-6 and Figures 9-1 through 9-5. Figures 9-2 and 9-3 also show data from the fission gas release model correlation data base as darkened symbols. As can be seen from these results, FATES3 does an excellent job of predicting these parameters. The individual data sets are further discussed below.

The fission gas release data of Bellamy and Rich (Refs. 9-1 and 9-2) were used as an independent check of the predictions of the C-E fission gas release model which is shown in Figure 9-1. These predictions were performed external to FATES3 with data as shown in Tables 9-5 and 9-6. The rods were irradiated for up to nine reactor cycles at DIDO in a sodium coolant. The clad operated at about 500°C, which is about 200°C higher than the typical operating temperature of Zircaloy cladding in commercial LWRs. Peak rod linear heat ratings ranged from an estimated 3 to 9 kw/ft, which were estimated to match the reported end-of-life fuel centerline temperatures. Gas release predictions have been made for 17 rods. These are the rods for which detailed fuel central temperature histories have been published by AERE, the test sponsor. These rods experienced a variety of duty cycles. Some had peak temperatures early in life while others had peak temperatures later or relatively constant thermal histories.

It is believed that for all rods in this experiment, even those with first cycle peaks in fuel temperature, the time-integrated release of fission gas can be predicted based on the reported fuel temperatures for the last irradiation cycle.

The reported temperatures are calculated values based on nonpublished rod linear heat ratings and the range of reported gap resistivity. The gap resistivity is reported to be between 1.5 and 2.0 cm^2 - °C/w (i.e., gap conductance between 0.5 and 0.667 w/cm^2 - °C). Tables 9-5 and 9-6 show the resulting range of predicted versus measured gas release values. The results are plotted in Figure 9-1.

The Petten data set, plotted in Figures 9-2 and 9-3, consists of short length rodlets of C-E and KWU design which were pre-irradiated in KWO and subsequently ramp tested in a pressurized capsule in the poolside facility of the Petten reactor in the Netherlands. The purpose of these tests was to measure pellet-clad interaction failure propensity. Extensive P.I.E. (Post Irradiation Examinations) was done on both failed and non-failed rods. Data from non-failed rods are an excellent source of fission gas release data for transient power conditions. Irradiation data and measured and predicted fission gas release values are given in Figure 9-4 for individual rodlets. All of the rodlets reported here did not fail during the ramp test.

The KWU rods were irradiated in the KWO and KKS reactors. There are standard full-length rods, experimental rods of high power with a high enrichment, and short length rods from a power cycling experiment in this data set. Due to this data being less well characterized as discussed in Section 9.1 the predicted results contain more scatter as would be expected.

The IFA 418 irradiation experiment is jointly sponsored by C-E and KWU at the Halden Boiling Water Reactor (HBWR) in Norway. The IFA 418 assembly consisted of six instrumented rods positioned in a circular array. Rods [ ] which contained C-E fabricated fuel, were selected for comparison. Fission gas release was measured [ ]. [ ] each contained a fuel centerline thermocouple (pellet ID = .07 in) in a short section of annular pellets at the bottom of the fuel stack. [ ] yielded fuel centerline temperature data out to burnups of [ ] Results of the fission gas release comparison is shown in Figures 9-2 and 9-3. Comparison of FATES3 temperatures with the thermocouple data is shown in Figures 9-4.

The IFA 428 irradiation experiment provided thermocouple data as shown on Figure 9-4. It is jointly sponsored by C-E and KWU at the HBWR. The IFA 428 assembly consisted of two six-rod clusters, one upper and one lower. C-E rods [ ] were selected for comparison. Each rod had two centerline thermocouples (pellet ID = .07 in), each extending about 4 inches into each end of the fuel stack. Fuel temperatures were recorded at regular intervals (which are shown on the figure) and were obtained out to about 3,200 MWD/MTU.

The IFA 11 and IFA 21 irradiation experiments (Ref. 9-3) were sponsored by AB Atomenergi at the HBWR. Each rod was equipped with a fuel centerline thermocouple (pellet ID = .05 in) extending about midway into the fuel stack. Four of six thermocouples yielded data only at beginning of life. The remaining two yielded data to 4,300 MWD/MTU. These rods are an older design, but are included because they have been historically used for temperature comparisons. Results of FATES3 predictions versus measured temperatures are also shown on Figure 9-4.

The Calvert Cliffs 1 rods were described in Section 2.5. They are used in this section to provide verification of predicted fuel rod internal void volume (or volume available for gases), which is important for calculating fuel rod internal pressure. These predicted and measured void volumes are at cold conditions and, therefore, give an excellent indication of expected changes

in internal pressure due to the irradiation induced changes in fuel rod dimensions (e.g., clad creepdown, fuel swelling, etc.). Results of the comparison between FATES3 and the measured data is shown in Figure 9-5. Agreement is excellent.

9.3 CONCLUSIONS

A comparison of FATES3 predictions with measured data have been made for fission gas release, fuel rod centerline temperature, and fuel rod internal void volume. Several conclusions may be drawn from these comparisons.

1. Predictions of fission gas release from UO_2 fuel using FATES3 agree quite well with measured data (which contain a wide variation in power levels and burnups) as shown in Figure 9-2. The more well-characterized the data the better the agreement, indicating an appropriate modeling of fission gas release mechanisms.

2. The burnup dependency of fission gas release is well modeled as shown by Figure 9-3. The data when normalized to burnup show no burnup trends for enhanced gas release beyond that inherent in the model.

3. FATES3 temperature predictions are shown in Figure 9-4 to be in fairly good agreement with measured data (but slightly high) through ~22000 MWD/MTU burnup. Fuel-clad gap closure has usually occurred at this burnup so uncertainties in temperature due to the effect of gap size on gap conductance are not present at higher burnups. This gives reasonable assurance that fuel temperatures at higher burnups will follow a similar trend.

4. The fuel rod internal void volume (available to accommodate fill gas and released fission gases) predicted by FATES3 is in excellent agreement with measured data to fairly high burnups. Therefore, prediction of fuel rod internal pressure would be expected to be excellent.

9.4 REFERENCES FOR SECTION 9.0

9-1 R. G. Bellamy and J. B. Rich, "Grain Boundary Gas Release and Swelling in High Burnup Uranium Dioxide", J. Nucl. Mat., 33 (1969) pp. 64-76.

9-2 Letter from R. G. Bellamy (AERE Harwell) to E. Roberts (W) dated March 13, 1975.

9-3 G. Kjaerheim and E. Rolstad, "In-Pile Determination of UO_2 Thermal Conductivity, Density Effects and Gap Conductance", HPR-80, December, 1967.

Table 9-1

Summary of Irradiation Parameters for
Rods in the Verification Data Base

Data	Number of Rods	Used For*	Peak Local Power (kw/ft)	Rod Average Burnup (MWD/KgU)
Petten	[			]
KWU				
Bellamy & Rich	17	F	3.1 - 8.7	8.0 - 47.8
IFA 418	[			]
IFA 428				
IFA 11 + 21	6	T	15.5	0 , 4.3
Calvert Cliffs 1	12	V	9.1 , 11.1	18.7 - 37.0

*

F - Fission gas release

T - Fuel temperature

V - Void volume

Table 9-2

Summary of Design Parameters
For Rods in the Verification Data Base

Parameter	Petten	KWU	Bellamy & Rich	IFA 418	IFA 428	IFA 11 & 21	Calvert Cliffs 1
Clad OD, in			.118-.236			.532-.541	.440
Clad ID, in			.330-.594			.496-.503	.388
Initial Pellet-Clad Dia. Gap, Mils			.001			1.9-6.6	8.5
Initial Grain Size, μm			12 , 15			14 , 25	2.5 - 15
Fuel Column Length, in			.8-1.2			67.5	136.7
Initial Fuel Density, % TD			95 , 98			96 , 98	93 - 95
Fill Gas Pressure* at 70°F, psia			---			15	315 , 465
Enrichment, %U235			---			5	2.5 , 2.8

[ ] the Bellamy & Rich rods which were fabricated in argon and helium atmospheres.

Table 9-3

Summary of Thermal-Hydraulic Parameters
For Rods in the Verification Data Base

Parameter	Petten*	KWU	Bellamy & Rich	IFA 418	IFA 428	IFA 11 & 21	Calvert Cliffs 1
Coolant Pressure, psia	[	]	---	[	]	420	2250
Coolant Inlet Temperature, ^{o}F	[	]	~900	[	]	450	548

*The coolant pressure and inlet temperature during power ramping are [ ] psia and [ ] respectively.

Table 9-4

Irradiation and Design Parameters for Petten Fuel Rods
with Measured and Predicted Fission Gas Release

Test Number	Initial Fuel Grain Size, μm	Ramp Peak LHGR, kw/ft*	Rod Average Burnup, MWD/KgU	Fission Gas Release, %	
				Measured	Predicted
[					]
[					
					]

TABLE 9-5

Comparison of Gas Release Model Predictions

with Data of Bellamy and Rich (Gap Resistivity = 2 cm^2-$^oC/w$)

Pin No.	Burnup Mwd/KgU	Fuel % TD	Fuel Grain Size, μm	Fuel Diam. cm	kw/ft	Fuel Surf. Temp., ^oC[a]	Fuel Central Temp., ^oC[b]	Pred. Gas Release, %	Exp. Gas Release, %
5020	8.0	95	12	0.594	6.22	719	1279	2.47	1.2
5036	17.5	95	12	0.594	8.66	805	1669	17.95	13.8
5026	19.3	95	12	0.482	6.42	778	1381	6.42	2.4
5042	30.0	95	12	0.482	7.87	841	1629	19.39	11.1
5033	13.6	98	15	0.470	6.40	784	1357	4.08	0.9
5030	13.9	98	15	0.374	4.16	732	1072	0.94	0.12
5029	14.1	98	15	0.330	3.15	699	943	0.39	0.09
5031	15.3	98	15	0.364	3.87	722	1033	0.74	0.16
5032	15.5	98	15	0.330	3.05	693	927	0.37	0.10
5037	18.2	98	15	0.330	3.15	699	943	0.45	0.2
5019	18.8	98	15	0.582	8.47	804	1602	11.13	1.5
5038	19.1	98	15	0.374	4.09	728	1061	1.02	0.2
5023	20.8	98	15	0.364	4.08	734	1068	1.13	0.22
5022	34.9	98	15	0.374	5.16	788	1238	3.90	2.52
5039	39.6	98	15	0.364	5.04	789	1228	3.97	3.1
5050	45.1	98	15	0.374	5.23	~ 792	~ 1250	4.70	4.1
5049	47.8	98	15	0.374	5.23	~ 792	~ 1250	4.81	7.1

[a] T_s (fuel surface, ^oC) = T_c (clad ID, ^oC) + 10.44 x kw/ft x Gap Resistivity (cm^2 - $^oC/w$) ÷ Pellet Diameter (cm)
where $T_c = 500^oC$

[b] Reported values of Refs 9-1 and 9-2.

TABLE 9-6

Comparison of Gas Release Model Predictions

with Data of Bellamy and Rich (Gap Resistivity = 1.5 cm^2-$^oC/W$)

Pin No.	Burnup Mwd/KgU	Fuel % TD	Fuel Grain Size, μm	Fuel Diam. cm	kw/ft	Fuel Surf. Temp., ^oC[a]	Fuel Central Temp., ^oC[b]	Pred. Gas Release, %	Exp. Gas Release, %
5020	8.0	95	12	0.594	6.03	659	1176	1.32	1.2
5036	17.5	95	12	0.594	8.87	734	1590	11.91	13.8
5026	19.3	95	12	0.482	6.19	701	1251	3.21	2.4
5042	30.0	95	12	0.482	7.71	751	1484	10.57	11.1
5033	13.6	98	15	0.470	6.19	706	1229	1.99	0.9
5030	13.9	98	15	0.374	3.96	665	971	0.43	0.12
5029	14.1	98	15	0.330	2.98	641	860	0.20	0.09
5031	15.3	98	15	0.364	3.58	654	925	0.31	0.16
5032	15.5	98	15	0.330	2.79	632	835	0.18	0.10
5037	18.2	98	15	0.330	3.04	644	869	0.25	0.2
5019	18.8	98	15	0.582	8.28	723	1466	6.39	1.5
5038	19.1	98	15	0.374	---	---	NA[c]	---	0.20
5023	20.8	98	15	0.364	3.87	666	965	0.51	0.22
5022	34.9	98	15	0.374	---	---	NA[c]	---	2.52
5039	39.6	98	15	0.364	5.12	720	1146	2.28	3.1
5050	45.1	98	15	0.374	---	---	NA[c]	---	4.1
5049	47.8	98	15	0.374	---	---	NA[c]	---	7.1

[a] T_s (fuel surface, ^oC) = T_c (clad ID, ^oC) + 10.44 x kw/ft x Gap Resistivity (cm^2 - $^oC/w$) ÷ Pellet Diameter (cm)
where $T_c = 500^oC$

[b] Reported values of Refs. 9-1 and 9-2

[c] Data Not Available

Figure 9-1

A Comparison of Model Predictions vs. Measured
Fission Gas Release for the Bellamy and Rich Data

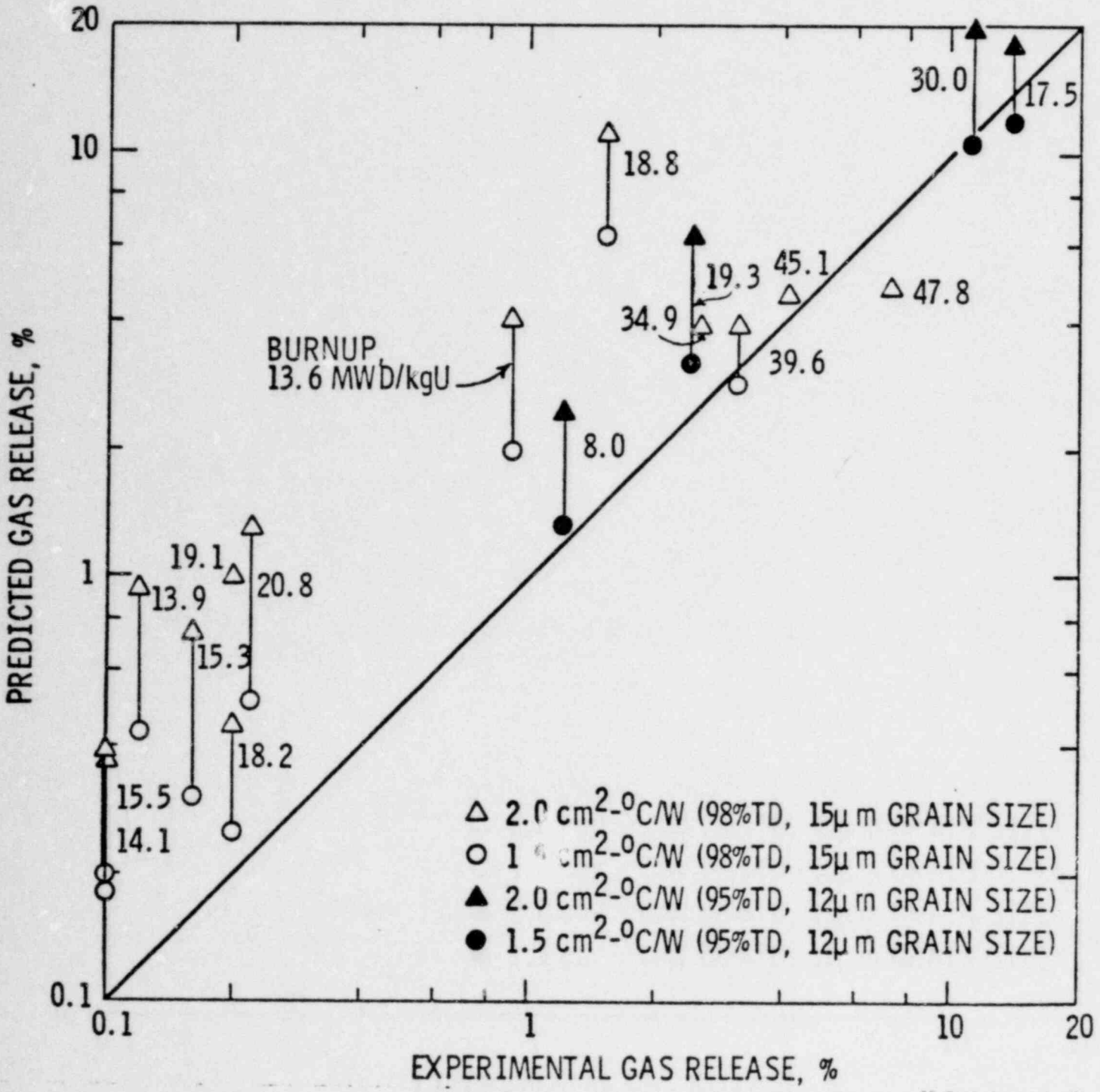

Figure 9-2
COMPARISON OF MEASURED AND PREDICTED FISSION GAS RELEASE

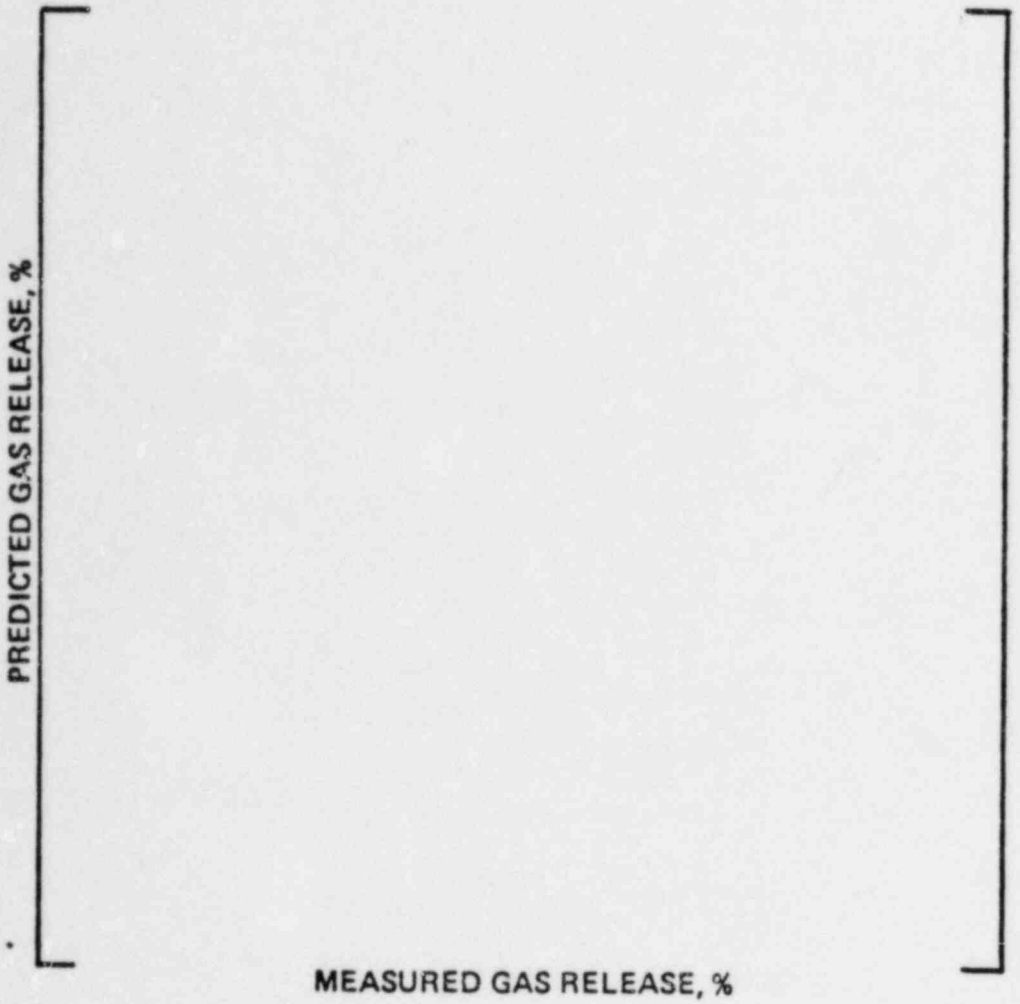

PREDICTED - MEASURED GAS RELEASE, %

BURNUP, MWD/KGU

Figure 9-3
PREDICTED - MEASURED GAS RELEASE VERSUS BURNUP

Figure 9-4

COMPARISON OF MEASURED AND PREDICTED FUEL CENTERLINE TEMPERATURES

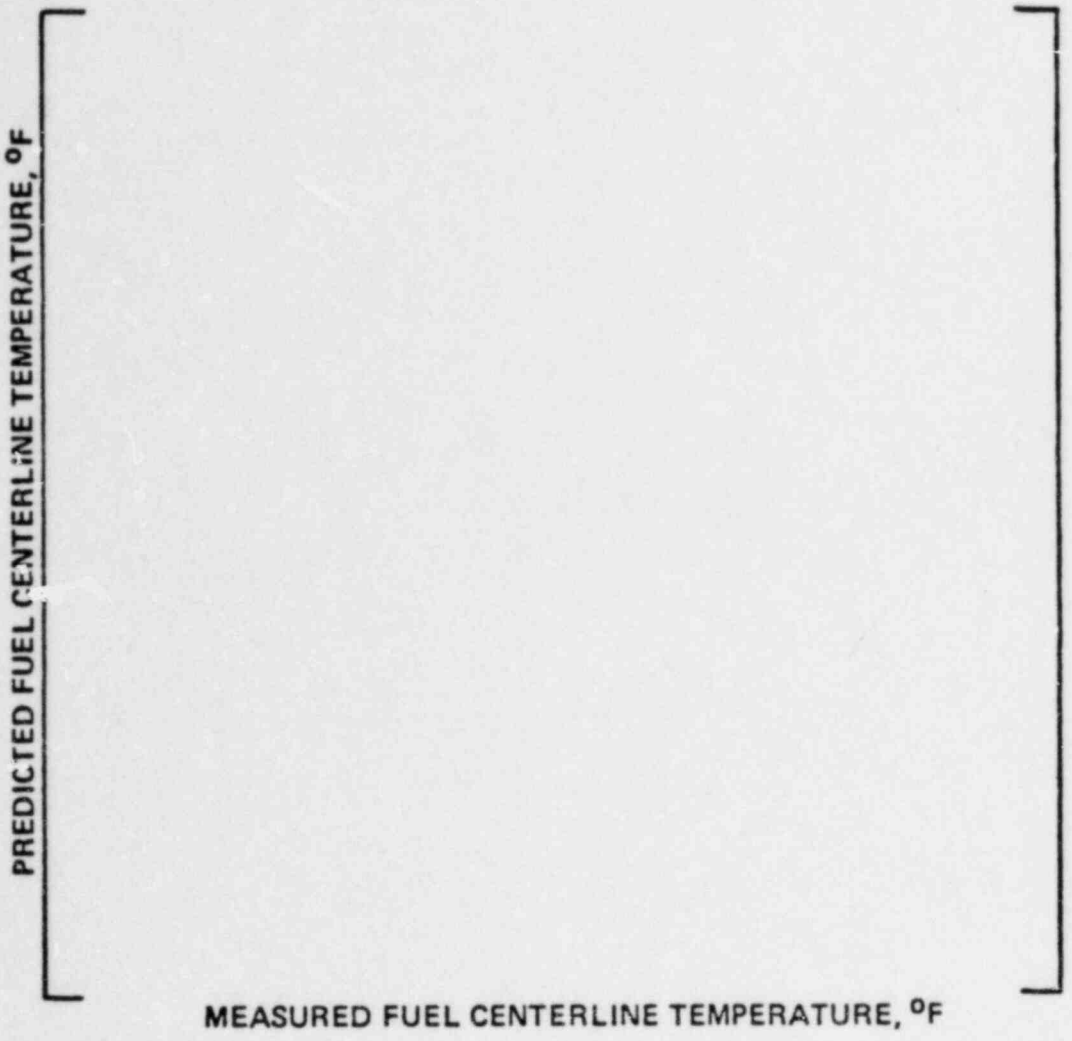

Figure 9-5
COMPARISON OF MEASURED AND PREDICTED VOID VOLUME
FOR CALVERT CLIFFS I TEST RODS